Optical probing of cold trapped atoms

R. W. Fox, S. L. Gilbert, L. Hollberg, and J. H. Marquardt

National Institute of Standards and Technology, Boulder, Colorado 80303

H. G. Robinson

Department of Physics, Duke University, Durham, North Carolina 27706

Received April 6, 1993

Transitions between excited states of laser-cooled and laser-trapped rubidium and cesium atoms are probed by use of fiber and diode lasers. High-resolution Doppler-free spectra are detected by observation of the absorption and fluorescence of light from the intermediate level of two-step cascade systems. The optical double-resonance spectra show Autler–Townes splitting in the weak probe limit and more complicated spectra for a strongly coupled three-level system.

The potential, and even the requirement, for the use of laser-cooled atoms in the highest-resolution optical spectroscopy is well recognized,[1] but little high-resolution optical spectroscopy has been done on laser-cooled neutral atoms. This is in marked contrast to impressive demonstrations of extremely high-resolution optical spectroscopy on laser-cooled trapped ions.[2] With room-temperature atoms and Doppler-free techniques such as saturated absorption and two-photon transitions, the ultimate resolution and spectroscopic accuracy is usually limited by velocity-dependent effects, such as transit time broadening, second-order Doppler shift, and wavefront curvature.[3] These limitations can be avoided by the use of low-velocity atoms. Trapped-atom systems also operate at low pressures, which should significantly reduce the pressure shifts that often plague gas-cell wavelength measurements and stability.

Two important technological advances have greatly simplified experiments with low-velocity atoms. These are magneto-optic traps[4] (also known as Zeeman-shift optical traps) and the implementation of these traps in a relatively simple vapor cell.[5] Recent research with neutral atom traps has demonstrated very-high-resolution microwave spectra,[6] narrow Raman spectra,[7] and optical spectroscopy out of the ground state.[8] To our knowledge, our experiments demonstrate the first high-resolution optical spectroscopy of excited states of laser-trapped and laser-cooled alkali atoms. By probing the excited state of the trapping transition, we have an independent diagnostic of the conditions of the trapped atoms.

In our experiments, cesium or rubidium atoms are trapped in separate vapor cells by use of diode lasers tuned to resonance lines of the atoms. Additional lasers are then used to probe the trapped atoms in the excited state of the trapping–cooling transition. The transitions of interest are shown on simplified energy-level diagrams in Fig. 1. Most of the experimental conditions are common to both systems and are similar to those described in the literature.[5,9] Small ion-pumped cell traps operate at background alkali pressures that range from 10^{-5} to 10^{-7} Pa ($\approx 10^{-7}$–10^{-9} Torr). The trapping laser beams are approximately 1 cm in diameter, with ~2–5 mW in each beam. In each experiment, an elliptically polarized probe beam copropagates with one of the trapping beams. These systems typically confine between 10^7 and 10^8 atoms in a 1–2-mm-diameter cloud at temperatures of a few hundred microkelvins.

The study of rubidium is part of a program to develop a wavelength standard for optical communications in the 1.5-μm region.[10] Atoms are trapped with the use of two 780-nm diode lasers. The trapping laser is tuned to the low-frequency side of the $5S_{1/2}$, $F = 2 \rightarrow 5P_{3/2}$, $F = 3$ rubidium (^{87}Rb) cycling transition and cools and traps the atoms. The repumping laser, tuned to the $5S_{1/2}$, $F = 1 \rightarrow 5P_{3/2}$, $F = 2$ transition, prevents the atoms from accumulating in the $F = 1$ ground state. The trapping laser was locked to the low-frequency side of the cooling transition by use of a signal from a saturated-absorption spectrometer. The 1.529-μm $5P_{3/2} \rightarrow 4D_{5/2}$ transitions were probed with the use of a tunable erbium-doped fiber laser that has a free-running linewidth of 1 MHz.[11] We observed these transitions by measuring their effect on the 780-nm trap fluorescence. When the fiber laser is tuned into resonance, it removes population from the $5P$, $F = 3$ level and

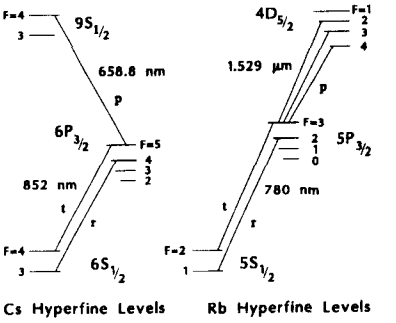

Fig. 1. Diagram of relevant energy levels of cesium (^{133}Cs) and rubidium (^{87}Rb) with the trapping–cooling (t), repumping (r), and probe (p) transitions indicated.

causes a reduction in the 780-nm fluorescent light emitted by the trapped atoms. The fiber laser's effect on this fluorescence can be quite large for the $5P$, $F = 3 \rightarrow 4D$, $F = 3$ and 2 transitions because it optically pumps the atoms into the $5S$, $F = 1$ state, removing them from the strongly fluorescing $5S$, $F = 2 \rightarrow 5P$, $F = 3 \rightarrow 5S$, $F = 2$ cycle. The atoms must then be pumped back into the cycling transition by the repumping laser. When the repumping rate is relatively small, this depopulation technique greatly enhances the sensitivity for detection of weak signals.[12] The $5P$, $F = 3 \rightarrow 4D$, $F = 4$ signal, however, is not enhanced because this transition does not optically pump the atoms into the $F = 1$ ground state. The $5S$, $F = 2$, $5P$, $F = 3$ and $4D$, $F = 4$ levels compose a closed system of three levels that are strongly coupled in the presence of the two laser fields. A small modulation was applied to the fiber-laser frequency, and the first derivative of the 780-nm trap fluorescence was obtained by use of phase-sensitive detection. Figure 2(a) shows this derivative signal as the 1.529-μm fiber laser is scanned through the resonances.

The trapped atoms in the cesium experiment are probed by observation of absorption out of the upper state of the $6S_{1/2}$, $F = 4 \rightarrow 6P_{3/2}$, $F = 5$ trapping–cooling transition. We used both direct absorption and derivative techniques to interrogate the red $6P_{3/2}$, $F = 5 \rightarrow 9S_{1/2}$, $F = 4$ transition at 658.8 nm. Approximately 1.5 mW of power at 658.8 nm was provided by an extended-cavity diode laser that was frequency stabilized to a reference cavity, resulting in a short-term linewidth of ~500 Hz. The laser's asymmetric spatial mode was filtered by a single-mode fiber used to deliver the light to the trap. The probe beam diameter was set to be approximately the same size as the trapped-atom cloud. After frequency stabilization, spatial filtering, and amplitude noise subtraction, the probe laser power at the trap was ~40 μW. Absorption by the trapped cesium atoms was typically 1% and provided a signal-to-noise ratio of ~10 in a 200-kHz detection bandwidth. The power in the probe laser is low enough so that it does not appear to perturb the trap dynamics or the absorption line shape. We accomplished precise detuning of the 852-nm cesium trapping laser by offset locking the laser (using an acousto-optic modulator) to a saturated-absorption crossover resonance. Figure 2(b) shows cesium absorption of the 658.8-nm probe light.

These cesium and rubidium cascade two-photon transitions have high signal-to-noise ratios and, because of the laser cooling, are free of Doppler broadening and associated effects. The obvious double-peaked nature of these signals is due to Autler–Townes splitting of the P states that is caused by the relatively strong trapping laser light.[13-15] The cesium $6P$, $F = 5 \rightarrow 9S$, $F = 4$ transition and the rubidium $5P$, $F = 3 \rightarrow 4D$, $F = 3$ and $F = 2$ transitions are representative of the moderately weak probe regime, in which the Rabi frequency owing to the probe light is much less than the Rabi frequency owing to the trapping laser. The $5P$, $F = 3 \rightarrow 4D$, $F = 4$ rubidium transition is in the moderately strong probe regime because of the larger matrix element for this transition. This strong coupling results in an asymmetic line shape. The observed linewidths are influenced by power broadening owing to the lasers, the magnetic-field gradient that causes splitting of the Zeeman levels, and nonuniform laser-field strength across the volume of the trap. From our measurements of linewidths with the magnetic field off, we conclude that broadening that results from the splitting of Zeeman levels is less than 1 MHz. We estimate that the residual Doppler broadening is less than 300 kHz. It is actually remarkable that the experimental line shapes are so narrow; linewidths as narrow as 3.1 MHz FWHM were observed on the 658.8-nm transition in cesium. This is to be compared with a natural width for the P state of 5.3 MHz. The ultimate probe transition linewidth is not affected by the intermediate-state lifetime; instead, it is limited by the natural linewidth of the upper level,[15] which is ~0.97 MHz for the $9S_{1/2}$ state of cesium and ~1.8 MHz for the $4D_{5/2}$ state of rubidium.

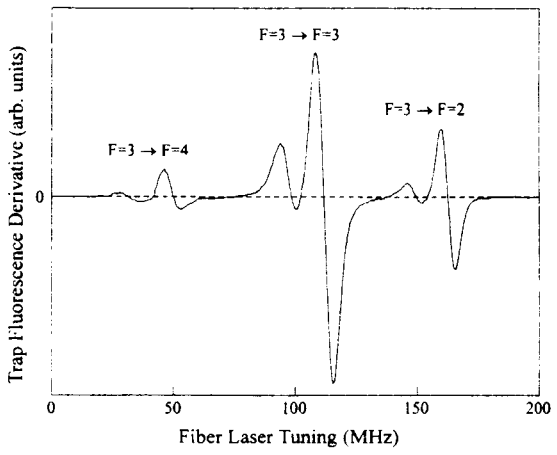

(a)

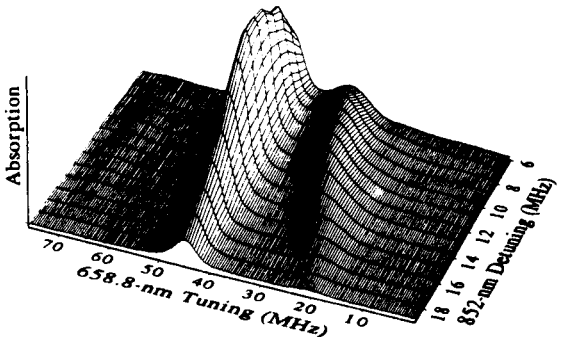

(b)

Fig. 2. (a) Rubidium line shape showing the derivative of the 780-nm fluorescence signal as the 1.529-μm fiber laser was scanned through the $5P_{3/2}$, $F = 3 \rightarrow 4D_{5/2}$, $F = 4$, 3, and 2 transitions. The trapping laser detuning was -11 ± 1 MHz, and the Rabi frequency was 8.5 ± 0.5 MHz. The fiber-laser intensity was 0.7 ± 0.2 mW/cm^2. (b) Cesium absorption at 658.8 nm as a function of the probe laser frequency for various trap laser detunings. We improved the signal-to-noise ratio by averaging 200 scans at each detuning. The large peaks on successive lines were aligned to display clearly the change in splitting.

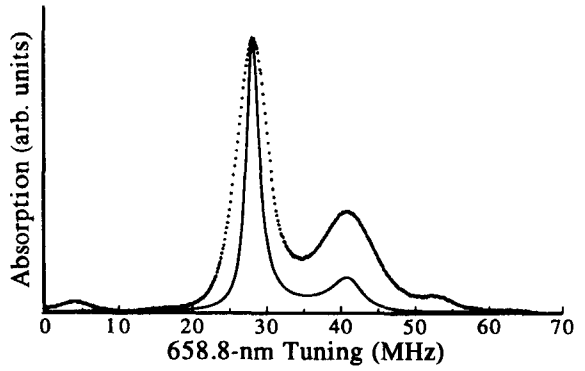

Fig. 3. Theoretical cesium-absorption line shape and experimental data points for 9-MHz detuning of the trapping laser and a Rabi frequency of 11 MHz. The experimental data show sidebands at 4 and 54 MHz that result from 25-MHz modulation of the probe laser. These sidebands are used for determining the frequency scale.

A density matrix model with five energy levels was used to calculate theoretical line shapes for the two-photon resonances. Three of these levels, $|1\rangle$, $|2\rangle$, and $|3\rangle$ with energies $E1 < E2 < E3$, form the cascade-level system that is coherently excited by two lasers. The remaining two levels, $|4\rangle$ and $|5\rangle$, are artificial levels that represent decay channels from $|2\rangle$ and $|3\rangle$ and can themselves decay only to the ground state $|1\rangle$. These artificial levels approximate the real effects of decay through other hyperfine levels and the repumping by a third laser. The parameters entering the theory include the trap laser detuning from resonance, the probe laser frequency (which was swept), the Rabi frequencies for the two applied laser fields, and the six relaxation coefficients between states. The relaxation coefficients and radiative decay constants come from known Einstein A values. Our analysis follows that of previous research[13] with some extensions.

To make the analysis tractable, we assume motionless atoms, uniform laser intensity, no collisions, and no trap dynamics. A simplified model of Zeeman broadening and magnetic-field gradients has been included. The general features of the theoretical line shape agree with the experimental results (see Fig. 3), but quantitative agreement is not found within experimental uncertainties. Our model contains no free parameters, other than signal size, and generally gives line shapes that are too narrow. Quantitative agreement of the line shapes should yield illuminating details of the dynamics of the trapped atoms, but will require more sophisticated models of the conditions within the trap. The most significant simplification in our model is the lack of averaging over the three-dimensional atom density and laser field and hence over the variation in Rabi frequency. These spatial variations may account for the difference between observed and calculated linewidths.

The potential accuracy in determining the line center in these narrow two-photon transitions is yet to be determined. Though essentially free from systematic effects owing to pressure, Doppler, transit, and wave-front perturbations, the transitions are affected by ac Stark shifts resulting from the trapping laser and, to a lesser extent, by the trap's magnetic field. These problems could be reduced by temporarily turning off the trapping fields while probing the atoms with weak laser fields.

These experiments have demonstrated the potential for high-resolution optical detection of narrow transitions in trapped neutral atoms. Experimental line shapes give good qualitative and fair quantitative agreement with calculations based on a simple model. Trapped neutral-atom spectroscopy yields Doppler-free signals and diagnostic information about the conditions of the trapped atoms; the Autler–Townes-split line shape provides information on the average square of the laser electric field that the atoms experience. As with trapped ions, we can anticipate that spectroscopy in these systems will soon measure resonances for which the accuracy and precision are not limited by the atom's environment.

We gratefully acknowledge the helpful comments of C. Wieman, C. Weimer, J. L. Hall, and J. Bollinger and the support of the U.S. Air Force Office of Scientific Research, NASA, and the Naval Command, Control and Ocean Surveillance Center.

References

1. J. L. Hall, M. Zhu, and P. Buch, J. Opt. Soc. Am. B **6,** 2194 (1989); W. Ertmer and S. Penselin, Metrologia **22,** 195 (1986).
2. J. C. Bergquist, W. M. Itano, F. Elsner, M. G. Raizen, and D. J. Wineland, in *Light Induced Kinetic Effects in Atoms, Ions and Molecules,* L. Moi, ed. (ETS Editrice, Pisa, Italy, 1991), p. 291; W. Nagourney, N. Ya, and H. Demelt, Opt. Commun. **79,** 176 (1990).
3. C. J. Bordé, J. L. Hall, C. V. Kunasz, and D. G. Hummer, Phys. Rev. A **14,** 236 (1976).
4. E. L. Raab, M. Prentiss, A. Cable, S. Chu, and D. Pritchard, Phys. Rev. Lett. **59,** 2631 (1987).
5. C. Monroe, W. Swann, H. Robinson, and C. Wieman, Phys. Rev. Lett. **65,** 1571 (1990).
6. C. Monroe, H. Robinson, and C. Wieman, Opt. Lett. **16,** 50 (1991); A. Clairon, C. Salomon, S. Guellati, and W. D. Phillips, Europhys. Lett. **16,** 165 (1991); K. Gibble and S. Chu, Phys. Rev. Lett. **70,** 1771 (1993).
7. D. Grison, B. Lounis, C. Salomon, J. Courtois, and G. Grynberg, Europhys. Lett. **15,** 149 (1991); J. Tabosa, G. Chan, and H. Kimble, Phys. Rev. Lett. **66,** 3245 (1991); L. Hilco, C. Fabre, and E. Giacobino, Europhys. Lett. **18,** 685 (1992).
8. M. Zhu, C. W. Oates, and J. L. Hall, Opt. Lett. **18,** 1186 (1993).
9. K. Lindquist, M. Stephens, and C. Wieman, Phys. Rev. A **46,** 4082 (1992).
10. S. L. Gilbert, Proc. Soc. Photo-Opt. Instrum. Eng. **1837,** 146 (1993).
11. S. L. Gilbert, Opt. Lett. **16,** 150 (1991).
12. D. J. Wineland and W. M. Itano, Phys. Lett. **82A,** 75 (1981).
13. S. H. Autler and C. H. Townes, Phys. Rev. **100,** 703 (1955); R. M. Whitley and C. R. Stroud, Jr., Phys. Rev. A **14,** 1498 (1976).
14. J. L. Picqué and J. Pinard, J. Phys. B **9,** L77 (1976).
15. P. R. Hemmer, B. W. Peuse, F. Y. Wu, J. E. Thomas, and S. Ezekiel, Opt. Lett. **6,** 531 (1981).